Screen-Space Normal Distribution Function Caching for Consistent Multi-Resolution Rendering of Large Particle Data
Supplementary Material

Mohamed Ibrahim, Patrick Wickenhäuser, Peter Rautek, Guido Reina, Markus Hadwiger

Abstract

This is the supplementary material for *Screen-Space Normal Distribution Function Caching for Consistent Multi-Resolution Rendering of Large Particle Data*.

1 Projected Solid Angle Measure

The *solid angle measure* $\sigma(\omega_m)$ corresponding to a solid angle ω_m around a normal $\mathbf{m} = (\theta, \phi)$ is given by (see Jakob [1] or Veach [2])

$$d\sigma(\omega_m) := \sin\theta \, d\theta \, d\phi, \tag{1}$$

which is the differential solid angle measure corresponding to the differential area $d\omega_m = \sin\theta \, d\theta \, d\phi$. The *projected* solid angle measure $\sigma^\perp(\omega_m)$ with respect to a fixed direction of projection $\mathbf{n}$ is then

$$d\sigma^\perp(\omega_m) = |\omega_m \cdot \mathbf{n}| \, d\sigma(\omega_m). \tag{2}$$

The (Lebesgue) integral of a function $f(\cdot)$ over a region $\mathscr{D} \subseteq \Omega$ on the hemisphere Ω with respect to the projected solid angle measure is

$$\int_{\mathscr{D}} f(\omega) \, d\sigma^\perp(\omega) := \int_{\mathscr{D}} f(\omega) \, |\omega \cdot \mathbf{n}| \, d\sigma(\omega). \tag{3}$$

In our case, the direction of projection $\mathbf{n}$ is usually either orthogonal to screen space, i.e., orthogonal to the output image plane, or it is a given normal direction $\mathbf{m}$. We observe that integration of the identity function ($f(\omega) := 1$) over the whole hemisphere Ω, with respect to the projected solid angle measure, yields the area of the unit disk $\Omega^\perp$:

$$\int_\Omega d\sigma^\perp(\omega) = \sigma^\perp(\Omega) = \pi. \tag{4}$$

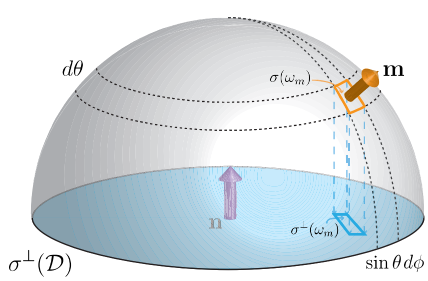

Figure 1: **Projected solid angle measure.** The projected solid angle measure $\sigma^\perp(\omega_m)$ for a solid angle ω_m about a direction $\mathbf{m}$ on Ω is the orthogonal projection of the solid angle ω_m onto $\Omega^\perp$, orthogonal to $\mathbf{n}$.

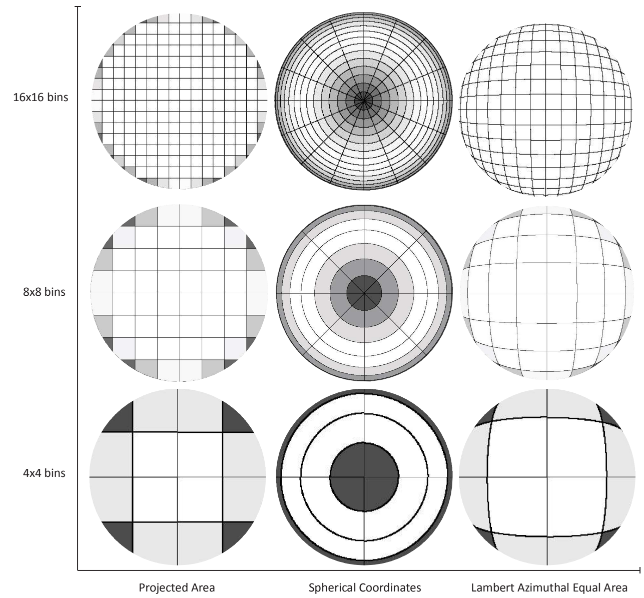

Figure 2: **Projected solid angle measure visualization.** We visualize the projected solid angle measure per bin for all of our three binning techniques using a different number of bins. The projected solid angle measures are color coded such that the brighter the color, the bigger the measure.

2 Filtering of Surface Normals

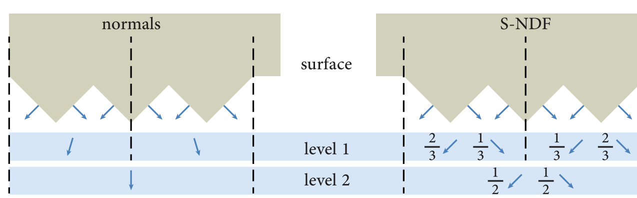

Figure 3: **Filtering of surface normals.** We observe a single pixel footprint that maps to complex surface geometry (a "v-groove" surface). These intricate details (i.e., surface normals) cannot be captured by linear filtering of the normals. Left: A linear combination (e.g., averaging) of all normals results in a single normal that does not represent the surface accurately. Right: For high-quality visualization, it is necessary to capture the entire *distribution* of surface normals in the pixel footprint, which leads to a screen-space normal distribution function (S-NDF) for this pixel.

3 S-NDF EXAMPLES

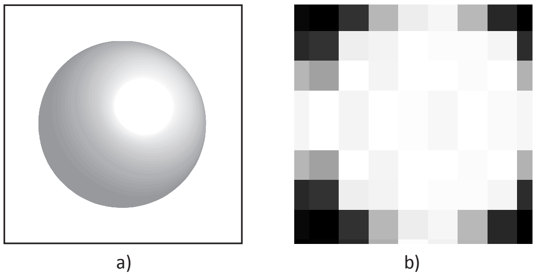

Figure 4: One Particle per Pixel: a) a pixel that sees one sphere, b) a visualization of the probabilities in the S-NDF bins of a pixel that sees one particle.

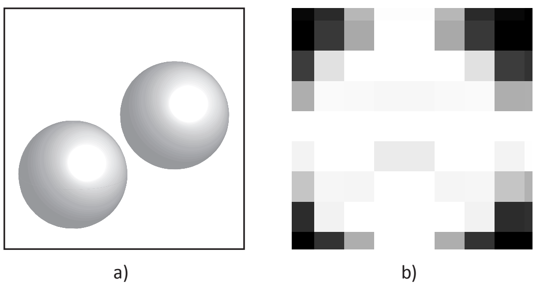

Figure 5: Two Non-Overlapping Particles per Pixel: a) a pixel that sees two non-overlapping spheres, b) a visualization of the probabilities in the S-NDF bins of a pixel that sees two non-overlapping particles.

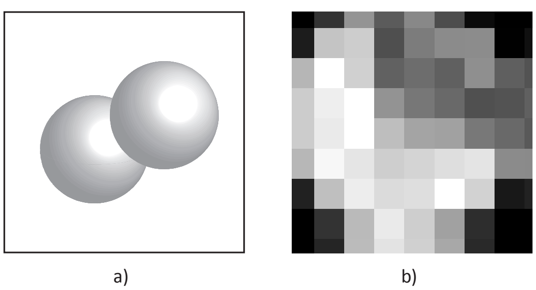

Figure 6: Two Overlapping Particles per Pixel: a) a pixel that sees two overlapping spheres, b) a visualization of the probabilities in the S-NDF bins of a pixel that sees two particles that overlap.

4 S-NDF DISCRETIZATION

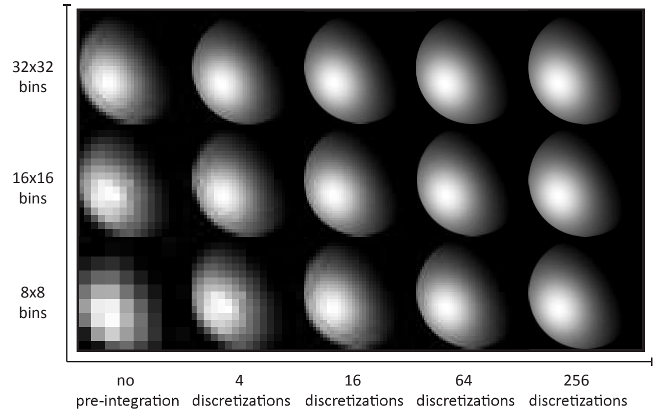

Figure 7: **Visualization of different S-NDF discretizations with and without pre-integration.** We render a transfer function using the Projected Normals binning technique using 64, 256, and 1024 bins (rows). For each bin, we show the rendering output with no pre-integration and with pre-integration using 4, 16, 64 and 256 discretizations.

5 Capturing Specularities

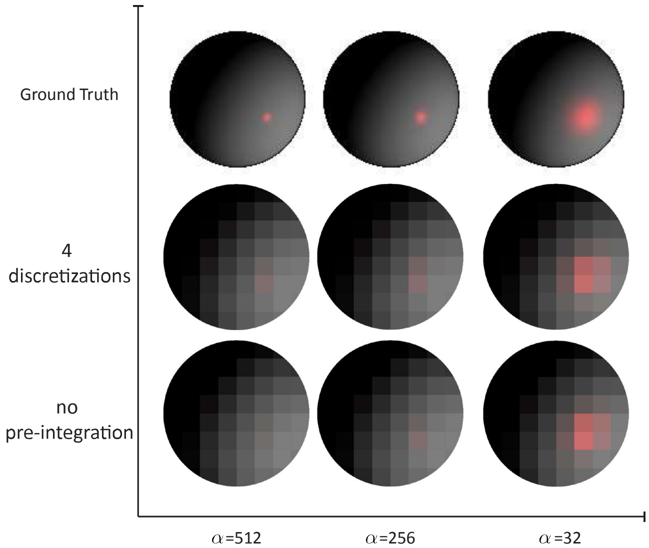

Figure 8: **Capturing specular highlights.** Pre-integration (with 4 dicretizations) helps with capturing small highlights as shown when the specular exponent α is high (512 and 256), when the specular exponent is low, the difference between the transfer functions with and without pre-integration is not noticeable.

6 Additional Results

References

[1] W. Jakob. *Light Transport on Path-Space Manifolds*. PhD thesis, Cornell University, 2013.

[2] E. Veach. *Robust Monte Carlo Methods for Light Transport Simulation*. PhD thesis, Stanford University, 1997.

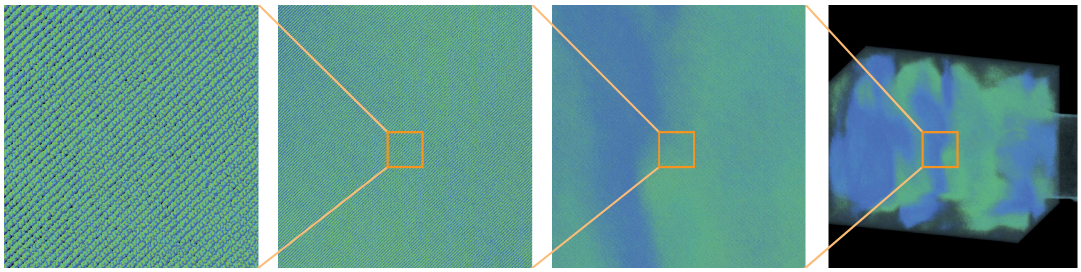

Figure 9: **Different zoom levels** of a large particle data set consisting of 48 million particles (laser ablation). On the left, individual sphere glyphs are clearly visible when zoomed into the data set, and aliasing is not an issue. From left to right: Our approach produces anti-aliased visualizations even when the particles become significantly smaller than a single pixel footprint, and the renderings are consistent across all zoom levels.

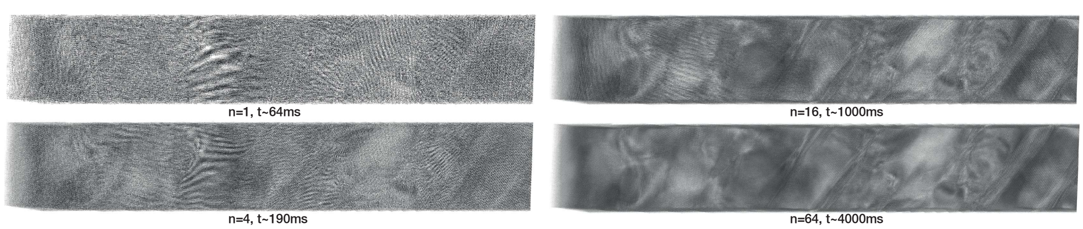

Figure 10: **Progressive refinement** of a large particle data set consisting of 12.5 million particles at an output resolution of 1920x1080 using one sample per pixel per progressive refinement iteration. n is the number of iterations (i.e., number of samples in each S-NDF), t the computation time.

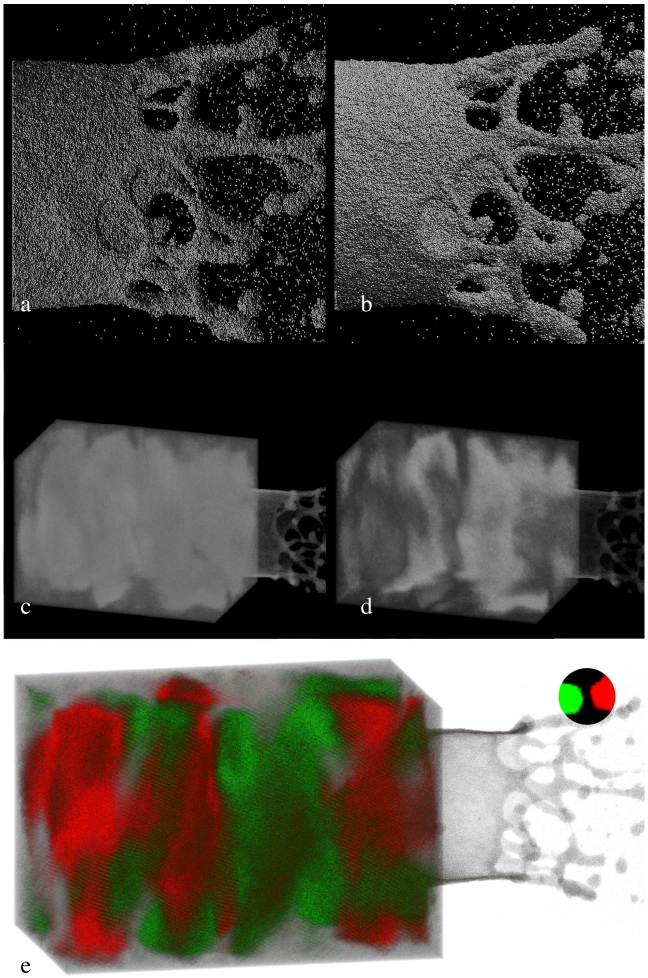

Figure 11: **Interactive exploration.** Close-ups (a) and (b), and overviews (c), (d), and (e), of the laser ablation data set. Images in one row use the same S-NDF, but are lit by different light sources. Because of orientation, some features are invisible under certain light directions (left), but are visible when moving the light source. The particle radius was increased in (a) and (b) to highlight mesoscopic features, while it was decreased in (d) and (e) to highlight the interior features that would otherwise be occluded. (e) uses a transfer function hand-drawn by the user during progressive refinement with real-time feedback from the visualization.